

Acknowledgements

We thank J. Flanagan, S. Prouty, S. Cutshall and D. Venzke for technical support. We also thank S. Weinstein for obtaining normal human muscle, T. Sudhof for the neuexin fusion protein complementary DNA, S. Froehner for the α -syntrophin antibody, and M. Oldstone for the DGFC5 construct. This work was supported by the Muscular Dystrophy Association and the National Institutes of Health (to S.A.M.). D.E.M. was supported by a Cardiovascular Interdisciplinary Research Fellowship and a University of Iowa Biosciences Initiative Fellowship. K.P.C. is an investigator of the Howard Hughes Medical Institute.

Competing interests statement

The authors declare that they have no competing financial interests.

Correspondence and requests for materials should be addressed to K.P.C. (e-mail: kevin-campbell@uiowa.edu).

Deletion of brain dystroglycan recapitulates aspects of congenital muscular dystrophy

Steven A. Moore*, Fumiaki Saito†, Jianguo Chen‡, Daniel E. Michele†, Michael D. Henry†, Albee Messing§, Ronald D. Cohn†, Susan E. Ross-Barta*, Steve Westra*, Roger A. Williamson||, Toshinori Hoshi‡ & Kevin P. Campbell†

* Department of Pathology; † Howard Hughes Medical Institute, Department of Physiology and Biophysics and Department of Neurology; ‡ Department of Physiology and Biophysics; and || Department of Obstetrics and Gynecology, The University of Iowa, Iowa City, Iowa 52242-1101, USA
§ Waisman Center and Department of Pathobiological Sciences, University of Wisconsin, Madison, Wisconsin 53705-2280, USA

Fukuyama congenital muscular dystrophy (FCMD), muscle–eye–brain disease (MEB), and Walker–Warburg syndrome are congenital muscular dystrophies (CMDs) with associated developmental brain defects^{1–4}. Mutations reported in genes of FCMD² and MEB⁵ patients suggest that the genes may be involved in protein glycosylation. Dystroglycan is a highly glycosylated component of the muscle dystrophin–glycoprotein complex⁶ that is also expressed in brain, where its function is unknown⁷. Here we show that brain-selective deletion of dystroglycan in mice is sufficient to cause CMD-like brain malformations, including disarray of cerebral cortical layering, fusion of cerebral hemispheres and cerebellar folia, and aberrant migration of granule cells. Dystroglycan-null brain loses its high-affinity binding to the extracellular matrix protein laminin, and shows discontinuities in the pial surface basal lamina (glia limitans) that probably underlie the neuronal migration errors. Furthermore, mutant mice have severely blunted hippocampal long-term potentiation with electrophysiologic characterization indicating that dystroglycan might have a postsynaptic role in learning and memory. Our data strongly support the hypothesis that defects in dystroglycan are central to the pathogenesis of structural and functional brain abnormalities seen in CMD.

The dystrophin–glycoprotein complex (DGC) of striated muscle is a well-characterized array of cytoplasmic, membrane-spanning and extracellular proteins that form a critical linkage between the cytoskeleton and the basal lamina⁸. The central protein linking DGC to the basal lamina is dystroglycan, a high-affinity receptor for several proteins (for example, laminin, agrin, neuexin and perlecan) that is composed of α - and β - subunits encoded by a single gene^{6,9}. α -dystroglycan (α -DG) is a highly glycosylated extracellular component, whereas β -DG spans the plasma membrane forming a

bridge between α -DG and the cytoskeleton⁶. Within the central nervous system (CNS), dystroglycan is abundant at two basal lamina interfaces formed by astrocytes: foot processes abutting on cerebral blood vessels, and foot processes that constitute the glia limitans at the pial surface of the brain and spinal cord⁷. Brain dystroglycan has also been localized to neuronal elements in several locations, including hippocampus and cerebellar cortex, where it may form a structural element of certain synapses⁷.

To explore the function of dystroglycan in brain and to determine whether dystroglycan operates in the pathogenesis of brain abnormalities such as those seen in CMD, we used Cre-loxP methodology to selectively delete dystroglycan from the CNS. Brain-selective expression of Cre recombinase was accomplished using a human glial fibrillary acid protein (GFAP) promoter expressed as early as embryonic day 13.5 (ref. 10). Studies in reporter mice reveal expression in astrocytes, oligodendroglia, ependyma and a large proportion of neurons¹⁰. It is likely that the human GFAP promoter is transiently active in neural progenitor cells, resulting in Cre recombination of floxed genes (genes flanked by loxP elements) that persist for the lifetime of several CNS cell lineages.

We produced both GFAP-Cre/DG^{lox/-} and GFAP-Cre/DG^{lox/lox} (GFAP-Cre/DG-null) mice that at weaning fit the expected mendelian distribution of each genotype. GFAP-Cre/DG-null mice are fertile and have no gross neurological abnormalities. Dystroglycan is largely absent from CNS tissue of GFAP-Cre/DG-null mice (Fig. 1a

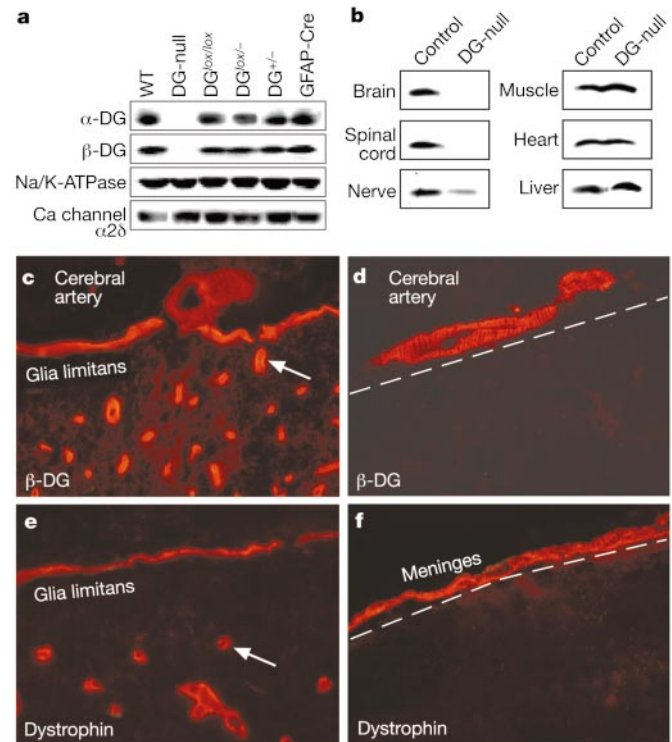


Figure 1 Tissue-selective deletion of dystroglycan. **a**, Western blot analysis of brain. WT, wild type; DG-null, GFAP-Cre/DG-null; DG^{+/-}, heterozygous dystroglycan null; DG^{lox/-}, heterozygous floxed/dystroglycan-null; DG^{lox/lox}, homozygous floxed. **b**, Western blot with a β -DG antibody. **c**, β -DG immunofluorescence of control cerebral cortex shows staining of smooth muscle in a small cerebral artery on the pial surface and astrocyte foot processes along the glia limitans and cerebral microvessels (arrow points to one microvessel). **d**, β -DG immunofluorescence is retained in only a small cerebral artery on the surface of DG-null cerebrum. **e**, Dystrophin immunofluorescence parallels that of β -DG in control brain. **f**, Dystrophin immunofluorescence is retained only in vessels of the meninges of DG-null brain. The position of the unstained glia limitans is marked by a dashed white line in **d** and **f**.

and Supplementary Information). Tissue-selective deletion of dystroglycan was verified by polymerase chain reaction (PCR) and western blotting, showing dystroglycan gene recombination and protein ablation only in brain, spinal cord and peripheral nerve (Fig. 1b and Supplementary Information). Immunofluorescence evaluation parallels the western blots and demonstrates the loss of dystroglycan from astrocytic foot processes abutting the glia limitans and cerebral microvessels (Fig. 1d). In addition to dystroglycan loss, dystrophin isoforms are not expressed at these pial and perivascular locations in GFAP-Cre/DG-null mice (Fig. 1f). This suggests that the absence of dystroglycan has disrupted the DGC at these sites. Dystroglycan and DGC expression is, however, main-

tained in vascular smooth muscle of cerebral blood vessels (Fig. 1d, f) and in choroid plexus (data not shown).

The loss of dystroglycan leads to a number of structural developmental defects in every GFAP-Cre-expressing brain examined on both DG^{lox/lox} and DG^{lox/-} backgrounds. These abnormalities range from macrocephaly to a variety of neuronal migration errors. An increase in brain size of nearly 20% is evident from gross observations and from comparing brain mass from GFAP-Cre/DG-null mice and their sex- and age-matched littermates ($P \ll 0.05$; see Supplementary Information). Histopathologic abnormalities similar, but not identical, to CMDs in the DG-null mice include fusion of the cerebral interhemispheric fissure and adjacent cerebellar folia, multifocal disarray of neuronal layering in the cerebral cortex, malformations resembling polymicrogyria, and relatively well-defined heterotopia within the superficial cortex (Fig. 2). Minor dispersion of neuronal cell bodies in the CA1 region and focal irregularities of the dentate granule cell layer are seen in the hippocampus of some DG-null mice, although major white-matter tracts are unremarkable (data not shown). All mice have well-formed corpus callosa, anterior cerebral arteries and lateral ventricles (Fig. 2b), thus distinguishing the midline fusion in DG-null mice from the malformation holoprosencephaly. Although foliation progresses in a reasonably normal fashion in DG-null mice (see

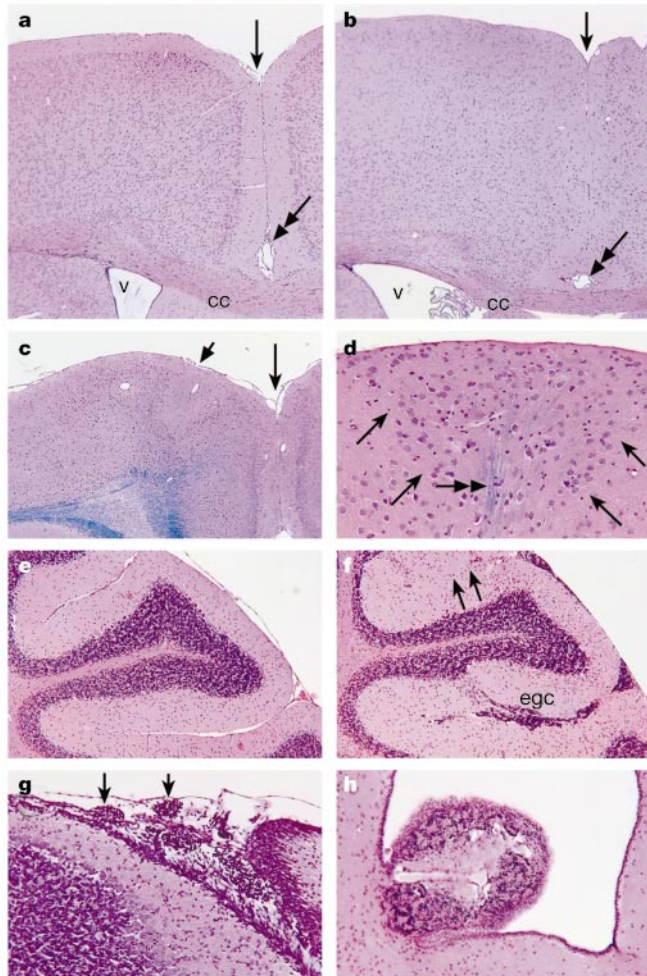


Figure 2 Abnormalities of cerebral and cerebellar development. **a**, Littermate control brain with normal interhemispheric fissure (vertical arrow), corpus callosum (cc), lateral ventricle (v) and anterior cerebral artery (double-headed arrow). **b**, GFAP-Cre/DG-null brain with fusion of the interhemispheric fissure, but normal corpus callosum, lateral ventricle and anterior cerebral artery. Abnormal neuronal migration has obscured the midline. Away from the midline there is disarray of cortical layering and migration of neurons into layer I, polymicrogyria (short arrow in **c**), and a distinct layer I heterotopia (outlined by single-headed arrows in **d**). A cluster of myelinated axons (double-headed arrow) passes through the cortex to this heterotopia. **e**, Para-sagittal section of control cerebellum. **f**, Para-sagittal section of GFAP-Cre/DG-null cerebellum shows abnormalities of external granule cell migration manifested by clusters of these neurons in one sulcus (egc) and along the pial surface (upper right area). There is fusion of another sulcus (arrows). **g**, Small clusters of external granule cells are abnormally placed in the subarachnoid space of a DG-null mouse at postnatal day 12 (arrows). **h**, Heterotopic cerebellar cortex forms a nodule protruding into the cerebral aqueduct of an adult DG-null mouse. **a, b, e-h**, Sections stained with haematoxylin and eosin. **c, d**, Sections stained with luxol fast blue.

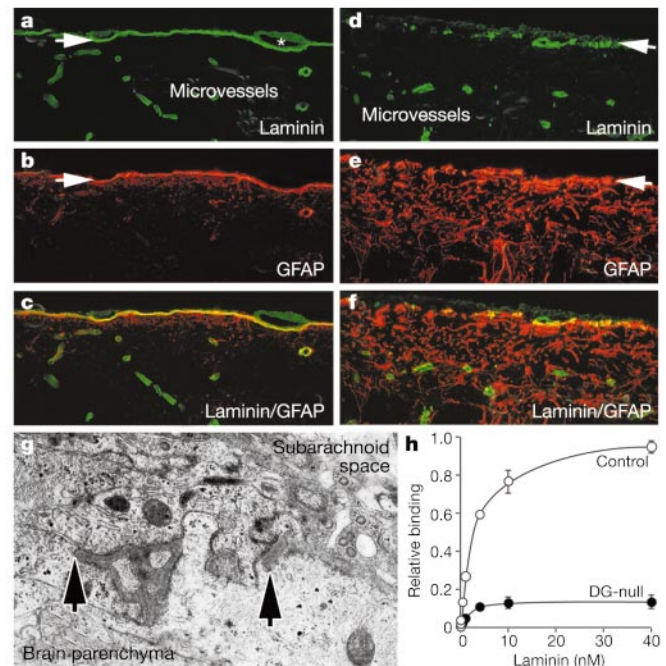


Figure 3 Disruptions of the glia limitans, leptomeningeal heterotopia and abnormal laminin binding. **a, d**, Laminin immunofluorescence (green) is present in the leptomeninges, pial vessels (asterisk in **a**), glia limitans (white arrows), and intracerebral microvessels of both control (**a**) and DG-null mice (**d**). The glia limitans is disrupted in DG-null mice (**d**). **b, e**, GFAP immunofluorescence (red) is prominent in only a superficial layer of astrocytes in control mice (**b**), but extends throughout the cortex in DG-null mice (**e**) (white arrows indicate glia limitans). **c, f**, Superimposing these images shows immunofluorescent overlap (yellow) between laminin and GFAP-stained astrocytic foot processes at the glia limitans and surrounding intracerebral blood vessels. Astrocytic processes extend through gaps in the glia limitans to form leptomeningeal heterotopia in DG-null mice (**f**). **g**, Electron microscopy confirms interruptions in the basal lamina of the glia limitans in DG-null mice (arrows), which should form a continuous horizontal band across the middle of this micrograph. Instead of being open, the subarachnoid space (upper portion of micrograph) is filled with cell processes. **h**, Total laminin binding is plotted for DG-null and littermate control brains. Binding in the absence of calcium was subtracted before plotting these curves.

Supplementary Information), there are residual nests of external granule cells in adult mice (Fig. 2f). Observations of granule cells in the subarachnoid space during postnatal cerebellar development in DG-null mice (Fig. 2g) suggest that abnormal migration and entrapment result in these granule cell nests. Additional heterotopic cerebellar tissue focally lines the subependymal regions of the fourth ventricle (see Supplementary Information) and forms nodules within the cerebral aqueduct (Fig. 2h).

Because dystroglycan is a major organizer of extracellular matrix proteins⁶, we hypothesized that the loss of dystroglycan from astrocyte foot processes at the glia limitans leads to basal lamina abnormalities that may underlie the neuronal migration errors present in our GFAP-Cre/DG-null mice. Indeed, immunofluorescence and ultrastructural analysis of both cerebral and cerebellar cortical surfaces of these mice reveals widespread discontinuities of the glia limitans accompanied by glial neuronal heterotopia within the leptomeninges (Fig. 3 and Supplementary Information; also see heterotopic granule cells in Fig. 2g). A profound reduction in the high-affinity laminin binding of DG-null brain (Fig. 3h) strongly suggests that the mechanism underlying the disruptions is a loss of ability to organize the basal lamina of the glia limitans. The basal lamina at this site is critical for normal cortical development. Enzymatic disruption or cold lesioning of this basal lamina causes abnormalities of cortical neuronal migration¹¹ and genetic disruption of perlecan or α 5-laminin, or combined disruption of α 3- and α 6-integrins, resulting in exencephaly, a severe defect in neural tube closure^{12–14}. Abnormalities of the glia limitans and meningeal heterotopia similar to our GFAP-Cre/DG-null mice have been reported after genetic deletion of β 1-integrin, another membrane protein closely associated with the extracellular matrix¹⁵. Interruption of glia limitans integrity in GFAP-Cre/DG-null mice may alter positioning cues or disrupt the radial glia scaffolding necessary for normal neuroblast migration¹⁶. And we cannot rule out the possibility that a loss of brain dystroglycan may also alter adhesion of neuroblasts to radial glia.

The human condition most closely resembling the GFAP-Cre/DG-null mice is type II (cobblestone) lissencephaly¹⁶, the common brain abnormality seen in some types of CMD^{1–4}. That mutations in several genes of the DGC lead to muscular dystrophy in humans and

animals⁸ has led to speculation that a member of the DGC may be responsible for both the dystrophy and the CNS abnormalities in these CMDs. This hypothesis has become more credible since the cloning of *fukutin*, the gene responsible for FCMD², and the discovery of *POMGnT1* mutations in MEB⁵. Although the precise function of fukutin is not known, comparison of its amino-acid sequence to those of other known proteins suggests that fukutin may be a secreted glycosyltransferase¹⁷. *POMGnT1*, however, is a glycosyltransferase enzyme that catalyses *O*-mannosyl glycosylation⁵. Additional linkages between muscular dystrophy and glycosyltransferases have been shown in *myd* mice and humans with the discovery of mutations in *LARGE* and fukutin-related protein, respectively^{18,19}. This molecular data and the accompanying observations of abnormal α -DG expression^{5,18–20} have brought greater attention to dystroglycan as a candidate target protein in CMD, despite the lack of direct evidence that any of these proteins glycosylate dystroglycan. Our study shows that deletion of brain dystroglycan is sufficient to cause brain developmental abnormalities similar to the type II lissencephaly seen in FCMD, Walker-Warburg syndrome and MEB^{4,16}. Thus, brain-selective deletion of dystroglycan provides strong experimental support for the hypothesis that dystroglycan abnormalities underlie the CNS abnormalities in this group of CMDs.

In an accompanying study²¹, the potential role of dystroglycan glycosylation in the pathogenesis of CMD is supported by new data derived from MEB and FCMD patients and from *myd* mice. Skeletal muscle from MEB, FCMD and *myd* has abnormalities of α -DG glycosylation and profound reductions in high-affinity laminin binding. Reduced laminin binding in the brains of *myd* mice is accompanied by disruptions of the glia limitans and neuronal migration errors markedly similar to those of GFAP-Cre/DG-null mice. Therefore, loss of dystroglycan function through either genetic deletion or abnormal post-translational modification results in brain pathology like that seen in CMD.

We were surprised at the prominence of GFAP-immunoreactive astrocytes in the cerebral cortex of GFAP-Cre/DG-null mice (Fig. 3e). Although identifying a cause for this ‘gliosis’ will require further evaluation, disruption of the glia limitans between the brain parenchyma and the subarachnoid space may be responsible. The glia limitans at its interface between cerebral spinal fluid and the brain is similar to Reichert’s membrane at its fetal–maternal interface in the developing embryo²². Both sites are proposed to provide a barrier and seem to have a high degree of dependence on dystroglycan for the development of a competent basal lamina. Loss of this glia limitans barrier, or perhaps abnormalities of the blood–brain barrier (another site from which astrocytic dystroglycan is lost), may lead to a reactive, inflammatory gliosis. Alternatively, altered neurogenesis or gliogenesis may underlie this striking astrocytic phenotype.

Dystroglycan is an important component of the neuromuscular junction, where it is proposed to organize postsynaptic components²³. Because dystroglycan is also localized to synaptic structures in sites such as the hippocampus⁷, we hypothesized that the broad deletion of dystroglycan from brains of these mice might alter synaptic function. Hippocampal slices prepared from 2–4-month-old GFAP-Cre/DG-null and littermate control mice were evaluated in a double-blind protocol that tested baseline neurotransmission, paired-pulse facilitation and long-term potentiation (LTP)—an electrophysiologic correlate of learning and memory²⁴. In control mice, robust LTP was consistently induced by high-frequency stimulation (HFS), whereas HFS induced only a short-term potentiation (STP) in the slices from DG-null mice (Fig. 4a). These results suggest that dystroglycan is required for HFS-induced LTP at CA3–CA1 synapses in the hippocampus.

In contrast to the blunted LTP, baseline neurotransmission was unaffected in the GFAP-Cre/DG-null mice (Fig. 4b). Stimulus–response relationships such as this are widely used to test the

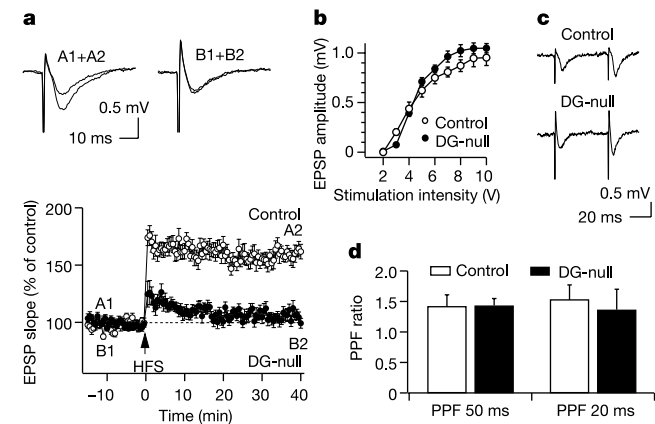


Figure 4 Long-term potentiation is blunted in GFAP-Cre/DG-null mice, but baseline neurotransmission and PPF are not affected. **a**, Representative EPSPs from control (A1, A2) and DG-null (B1, B2) mice (top). HFS induced LTP in control mice, but failed to induce LTP in DG-null mice. The slopes of the EPSPs before HFS served as control. The normalized slopes of EPSPs are plotted as a function of time. **b**, The stimulus–response curves from control and DG-null mice were produced by plotting the EPSP amplitudes against stimulation intensity. **c**, Representative raw PPF traces at 50-ms pulse intervals from control and DG-null mice. **d**, Averaged PPF ratios at 50- and 20-ms pulse intervals from control and DG-null mice.

properties of synaptic neurotransmission. Normal neurotransmission was observed despite the sporadic occurrence of the minor errors in hippocampal neuronal migration described above.

To determine whether the dystroglycan effect on LTP might be related to pre- or postsynaptic events, paired-pulse facilitation (PPF) was used to assess presynaptic neurotransmitter release²⁵. PPF with intervals of 50 and 20 ms did not differ significantly from each other in control and DG-null mice (Fig. 4c, d). These results indicate that the deficiency of dystroglycan does not affect presynaptic neurotransmitter release, and suggest that dystroglycan may contribute to the induction of LTP through an alternative, possibly postsynaptic, mechanism. This localization suggests a role for dystroglycan in CNS synapses similar to its role at the neuromuscular junction, where dystroglycan is proposed to organize the postsynaptic site^{6,23}. Alternatively, a growing literature indicating that astrocytes may integrate synaptic function²⁶ suggests that astrocyte abnormalities resulting from the loss of dystroglycan may account for the observed blunting of LTP in DG-null mice. □

Methods

Generation of floxed dystroglycan mice

A floxed DG targeting construct was generated with a floxed PGK-neo vector²⁷ that results in the insertion of a floxed *neo* cassette at the *Sall* site in the intron 5' of exon 2 and a *loxP* site at an *EcoRV* site 3' of exon 2, at a distance from the polyadenylation signal sequence (see Supplementary Information). This vector was electroporated into R1 embryonic stem cells and targeted clones were used to generate chimaeric animals. Germline transmission of the floxed DG allele was established by Southern blot and PCR screening of agouti offspring. Mice bearing the floxed DG allele were mated to the GFAP-Cre mice¹⁰.

Histology and immunohistochemistry

Histopathological studies were performed on mice of ages between postnatal day 12 and 52 weeks using standard haematoxylin and eosin, luxol fast blue, and Nissl staining methods. Tissues for electron microscopy were dissected from mice after transcardiac perfusion with 4% paraformaldehyde in PBS. Immunofluorescence was carried out on frozen sections using: polyclonal antibody against β -dystroglycan (rabbit 83)²⁸; monoclonal antibodies against dystrophin (MANDRA1) and GFAP (GFAP-Cy3) (Sigma); monoclonal antibody against α -dystroglycan (IH6)²⁹; and polyclonal antibody against laminin (Sigma). Appropriately labelled secondary antibodies were obtained from Molecular Probes.

Biochemical analysis

Fresh tissue was disrupted sequentially by polytron and Dounce homogenization in 20 mM PBS, pH 7.1, 0.3 M sucrose, 1 mM MgCl₂, 0.5 mM EDTA, 0.6 mg ml⁻¹ pepstatin A, 0.5 mg ml⁻¹ leupeptin, 0.5 mg ml⁻¹ aprotinin, 0.75 mM benzamidin, 0.1 mM phenylmethyl sulphonyl fluoride, 0.4 mg ml⁻¹ calpain inhibitor 1, 0.4 mg ml⁻¹ calpeptin (Buffer A). The homogenate was centrifuged at 13,800g for 23 min at 4°C. The supernatant was centrifuged at 31,000g for 35 min at 4°C and the pellet was resuspended with Buffer A and subjected to SDS-polyacrylamide gel electrophoresis as a microsome fraction. Proteins were resolved by SDS-PAGE on 3–12% linear-gradient gels. Transfers were incubated with primary antibodies (α - and β -dystroglycan antibodies, as described above, Na/K-ATPase, and calcium channel, α 2 δ ^{28,29}) followed by appropriate peroxidase-conjugated secondary antibodies and developed using enhanced chemiluminescence (Super Signal, Pierce).

For laminin binding, 100 mg of mouse muscle or brain were solubilized in 1 ml of Tris-buffered saline (TBS) containing 1% Triton X-100 and protease inhibitors, and briefly centrifuged. Wheat germ agglutinin eluates were diluted 1:50 in TBS and coated on polystyrene enzyme-linked immunosorbent assay microplates (Costar) where binding assays with mouse Engelbreth-Holm-Swarm (EHS) laminin were carried out (see ref. 21).

Electrophysiology

Transverse hippocampal slices (350–400 μ m) from bregma -2.2 to -3.6 were prepared from control ($n = 8$) and GFAP-Cre/DG-null ($n = 9$) littermates at 2–4 months old, then studied without knowledge of the genotype. The brains were sectioned in ice-cold artificial cerebrospinal fluid at pH 7.4 containing (in mM): 119 NaCl, 2.5 KCl, 2.5 CaCl₂, 1.0 NaH₂PO₄, 1.3 MgSO₄, 26.2 NaHCO₃, 11 glucose, bubbled with 95% O₂ with 5% CO₂, and the slices incubated in the same solution at 31°C for 2–5 h before recording.

Standard extracellular field potential recordings were performed at 31 ± 0.5 °C³⁰. Field postsynaptic excitatory potentials (EPSPs) were evoked in CA1 stratum radiatum by stimulation of Schaffer collaterals with a bipolar electrode placed at the border of CA3–CA1 and recorded with a 3 M NaCl-filled glass pipette (<5 M Ω) using a biological amplifier (WPI, Iso-DAM8). Stimulation (100 μ s) was delivered every 30 s by a stimulus isolation unit (Grass, SD9). Stimulus-response curves were obtained by plotting the stimulus voltages against the amplitudes of the EPSPs. LTP was induced by a high-frequency stimulation (HFS; 100 Hz, 1 s) and was measured by normalizing the EPSP slopes after HFS to the mean slope of the baseline EPSP before HFS. Paired-pulse facilitation was observed by applying paired pulses with a 50- or 20-ms interval. Data were digitized (10 kHz), filtered at 1 kHz, monitored online, and stored for later analysis by

Pulse 8.41 (HEKA). The offline analysis was performed by PatchMachine (<http://www.hoshi.org>) and IgorPro version 4.0 (WaveMetrics). Unless otherwise noted, two-sample Student's *t*-tests were used to calculate the statistical significance.

Received 8 January; accepted 22 April 2002; doi:10.1038/nature00838.

1. Fukuyama, Y., Osawa, M. & Suzuki, H. Congenital progressive muscular dystrophy of the Fukuyama type—clinical, genetic and pathological considerations. *Brain Dev.* **3**, 1–29 (1981).
2. Kobayashi, K. *et al.* An ancient retrotransposon insertion causes Fukuyama-type congenital muscular dystrophy. *Nature* **394**, 388–392 (1998).
3. Cormand, B. *et al.* Clinical and genetic distinction between Walker-Warburg syndrome and muscle-eye-brain disease. *Neurology* **56**, 1059–1069 (2001).
4. Haltia, M. *et al.* Muscle-eye-brain disease: a neuropathological study. *Ann. Neurol.* **41**, 173–180 (1997).
5. Yoshida, A. *et al.* Muscular dystrophy and neuronal migration disorder caused by mutations in a glycosyltransferase, POMGnT1. *Dev. Cell* **1**, 717–724 (2001).
6. Henry, M. D. & Campbell, K. P. Dystroglycan inside and out. *Curr. Opin. Cell Biol.* **11**, 602–607 (1999).
7. Zaccaria, M. L., di Tommaso, F., Brancaccio, A., Paggi, P. & Petrucci, T. C. Dystroglycan distribution in adult mouse brain: a light and electron microscopy study. *Neuroscience* **104**, 311–324 (2001).
8. Cohn, R. D. & Campbell, K. P. The molecular basis of muscular dystrophy. *Muscle Nerve* **23**, 1456–1471 (2000).
9. Sugita, S. *et al.* A stoichiometric complex of neuexins and dystroglycan in brain. *J. Cell Biol.* **154**, 435–445 (2001).
10. Zhuo, L. *et al.* hGFAP-cre transgenic mice for manipulation of glial and neuronal function in vivo. *Genesis* **31**, 85–94 (2001).
11. Choi, B. H. Role of the basement membrane in neurogenesis and repair of injury in the central nervous system. *Microsc. Res. Tech.* **28**, 193–203 (1994).
12. Arikawa-Hirasawa, E., Watanabe, H., Takami, H., Hassel, J. R. & Yamada, Y. Perlecan is essential for cartilage and cephalic development. *Nature Genet.* **23**, 354–358 (1999).
13. De Arcangelis, A., Mark, M., Kreidberg, J., Sorokin, L. & Georges-Labouesse, E. Synergistic activities of α 3 and α 6 integrins are required during apical ectodermal ridge formation and organogenesis in the mouse. *Development* **126**, 3957–3968 (1999).
14. Miner, J. H., Cunningham, J. & Sanes, J. R. Roles for laminin in embryogenesis: exencephaly, syndactyly, and placentopathy in mice lacking the laminin α 5 chain. *J. Cell Biol.* **143**, 1713–1723 (1998).
15. Graus-Porta, D. *et al.* β 1-class integrins regulate the development of laminae and folia in the cerebral and cerebellar cortex. *Neuron* **31**, 367–379 (2001).
16. Ross, M. E. & Walsh, C. A. Human brain malformations and their lessons for neuronal migration. *Annu. Rev. Neurosci.* **24**, 1041–1070 (2001).
17. Aravind, L. & Koonin, E. V. The fukutin protein family—predicted enzymes modifying cell-surface molecules. *Curr. Biol.* **22**, R837–R837 (1999).
18. Grewal, P. K., Holzfeind, P. J., Bittner, R. E. & Hewitt, J. E. Mutant glycosyltransferase and altered glycosylation of α -dystroglycan in the myodystrophy mouse. *Nature Genet.* **28**, 151–154 (2001).
19. Brockington, M. *et al.* Mutations in the Fukutin-related protein gene (*FKRP*) cause a form of congenital muscular dystrophy with secondary laminin α 2 deficiency and abnormal glycosylation of α -dystroglycan. *Am. J. Hum. Genet.* **69**, 1198–1209 (2001).
20. Hayashi, Y. K. *et al.* Selective deficiency of α -dystroglycan in Fukuyama-type congenital muscular dystrophy. *Neurology* **57**, 115–121 (2001).
21. Michele, D. E. *et al.* Post-translational disruption of dystroglycan–ligand interactions in congenital muscular dystrophies. *Nature* **418**, 417–422 (2002).
22. Williamson, R. A. *et al.* Dystroglycan is essential for early embryonic development: disruption of Reichert's membrane in Dag1-null mice. *Hum. Mol. Genet.* **6**, 831–841 (1997).
23. Grady, M. *et al.* Maturation and maintenance of the neuromuscular synapse: genetic evidence for roles of the dystrophin–glycoprotein complex. *Neuron* **25**, 279–293 (2000).
24. Bliss, T. V. P. & Collingridge, G. L. A synaptic model of memory: long-term potentiation in the hippocampus. *Nature* **361**, 31–39 (1993).
25. Schulz, P. E., Cook, E. P. & Johnston, D. Changes in paired-pulse facilitation suggest presynaptic involvement in long-term potentiation. *J. Neurosci.* **14**, 5325–5337 (1994).
26. Haydon, P. A. Glia: listening and talking to the synapse. *Nature Rev. Neurosci.* **2**, 185–193 (2001).
27. Potocnik, A. J., Brakebusch, C. & Fässler, R. Fetal and adult hematopoietic stem cells require β 1 integrin function for colonizing fetal liver, spleen, and bone marrow. *Immunity* **6**, 653–663 (2000).
28. Duclos, F. *et al.* Progressive muscular dystrophy in α -sarcoglycan-deficient mice. *J. Cell Biol.* **142**, 1461–1471 (1998).
29. Ervasti, J. M. & Campbell, K. P. A role for the dystrophin–glycoprotein complex as a transmembrane linker between laminin and actin. *J. Cell Biol.* **122**, 809–823 (1993).
30. Malenka, R. C. Postsynaptic factors control the duration of synaptic enhancement in area CA1 of the hippocampus. *Neuron* **6**, 53–60 (1991).

Supplementary Information accompanies the paper on Nature's website (<http://www.nature.com/nature>).

Acknowledgements

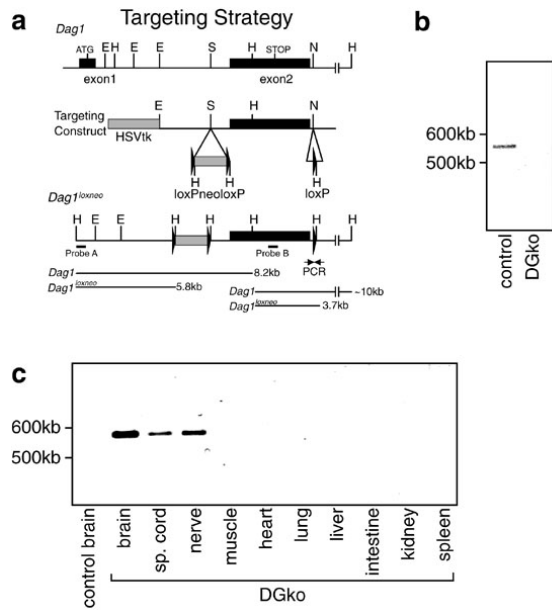
We thank R. Fässler for his gifts of plasmids for construction of the floxed allele. Technical assistance was received from J. Carl, C. Bromley, J. Rogers, C. Bray, M. Hassebrock, S. Lowen and K. Garringer. This work was supported by the Muscular Dystrophy Association and the National Institutes of Health (to S.A.M.). K.P.C. is an Investigator of the Howard Hughes Medical Institute.

Competing interests statement

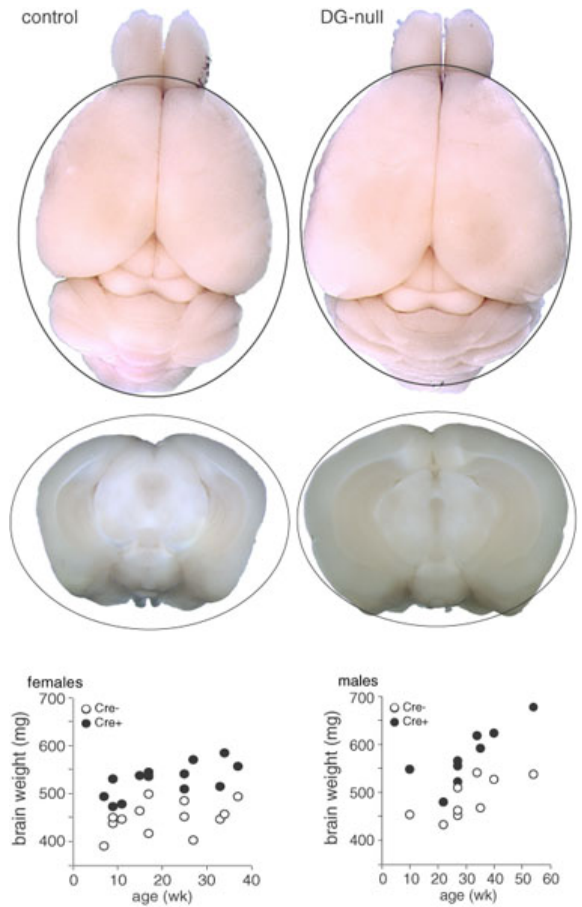
The authors declare that they have no competing financial interests.

Correspondence and requests for materials should be addressed to K.P.C. (e-mail: kevin-campbell@uiowa.edu).

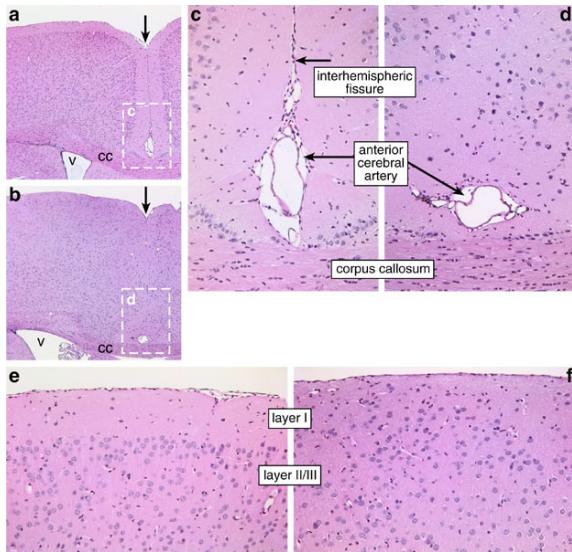
Supplemental Experimental Procedures



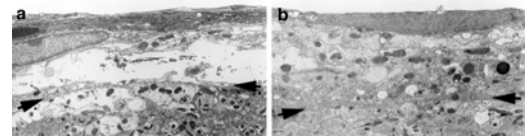
Supplemental Figure 1 a, Design of floxed dystroglycan mice. b, Dystroglycan rTPCR from total brain RNA. Gene specific sense primer (5'-GCTCATTTCGAGTGAGCATTC-3') and antisense primer (5'-CTAGTTTCCAGGACAGGAGA-3') were designed to anneal to the sequences in exon 1 and exon 2, respectively. c, Tissue-selective recombination of floxed dystroglycan gene. Gene specific sense primer (5'-CGAACACTGAGTTCATCC-3') and antisense primer (5'-CAACTGCTGCATCTAC-3') were designed to anneal to the intronic sequences flanking exon 2, which allow amplification of a 585 bp fragment only when exon 2 and the neo cassette are excised by Cre recombinase.



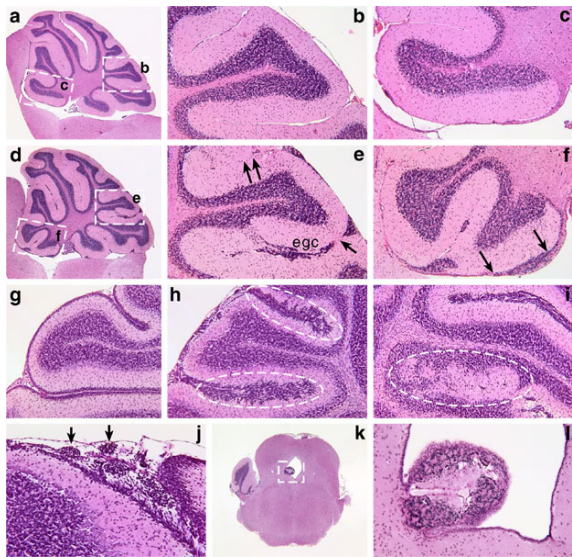
Supplemental Figure 2 Macrocephaly. Photographs are from littermate control and GFAP-Cre/DG-null mice (dorsal surfaces and coronal sections). Graphs are brain weights from littermate pairs. Brain weights are increased by 17.7% in DG-null females ($p=0.00002$; 13 littermate pairs) and by 18.2% in DG-null males ($p=0.00004$; 9 littermate pairs). Brain/body weight ratios are also increased in DG-null mice (20.5% increase in females, $p=0.009$; 30.3% increase in males, $p=0.008$).



Supplemental Figure 3 Cerebral neuronal migration abnormalities. H&E stained sections from littermate control (a, c, and e) and GFAP-Cre/DG-null (b, d, and f) mice show midline fusion (vertical arrows), disarray of neuronal migration, and normal location of anterior cerebral artery, corpus callosum (cc), and lateral ventricle (v).



Supplemental Figure 5 Glial-neuronal meningeal heterotopia. Electron micrographs from littermate control and GFAP-Cre/DG-null mice. The normally open subarachnoid space (a) is filled with heterotopic astrocytic and neuronal processes in DG-null mice (b). Arrows mark the location of the glia limitans in each micrograph. Brain parenchyma is at the bottom of each micrograph.



Supplemental Figure 4 Cerebellar and brain stem neuronal migration abnormalities. H&E stained sections from littermate control (a, b, c, and g) and GFAP-Cre/DG-null (d, e, f, h, i, and j) cerebella and DG-null brain stem (k and l). Arrows in (e) mark fusion of adjacent folia, while arrows in (f) show subependymal, heterotopic cerebellar cortex. Regions of abnormal granule cell migration are labeled "egc" in (e) and marked by dashed white ovals in (h) and (i) or arrows in (j). Panels a-f, k and j are from adult mice. Panels g-j are from postnatal day 12 mice.